LITERATURE CITED

Brian, P. L. T., "Engineering for Pure Water—Part II: Freezing," *Mech. Eng.*, **90**, 42 (1968).

Barduhn, A. J., "The Freezing Process for Water Conversion in the United States," *Proceedings, First International Symposium on Water Desalination*, Washington, D.C., October 3-9, 1965, U.S Department of Interior, **2**, 641 (1967).

Bosworth, C. M., S. A. Carfagno, and D. J. Sandell, Office of Saline Water Research and Development Progress Report No. 23, U.S. Department of Interior (1959).

Bosworth, C. M., A. J. Barduhn, S. A. Carfagno, and D. J. Sandell, Office of Saline Water Research and Development Progress Report No. 32, U.S. Department of Interior (1959).

Hahn, W. J., R. C. Burns, R. S. Fullerton, and D. J. Sandell, Office of Saline Water Research and Development Progress Report No. 113, U.S. Department of Interior (1964).

Mixon, F. O., "Calculation of Liquid Flow Path in a Rectangular Wash-Separator Column with Vertical Filter Screens," Research Triangle Institute Report on OSW Contact 379 (1964).

Hahn, W. J., "Countercurrent Wash Separation Column Design," *OSW Symposium on Freezing and Ion Adsorption*, Hollywood, California, (Nov. 15-17, 1965). (Not published)

Wiegandt, H. F., Office of Saline Water Research and Development Progress Report No. 41, U.S. Department of Interior (1960).

Consie, R., D. Emmermann, J. Fraser, W. B. Johnson, and W. E. Johnson, Office of Saline Water Research and Development Progress Report No. 295, U.S. Department of Interior (1968).

Sherwood, T. K., P. L. T. Brian, A. F. Sarofim, and K. A. Smith, Office of Saline Water Research and Development Progress Report No. 436, U.S. Department of Interior (1969).

Shwartz, J., and R. F. Probstein, "An Analysis of Counterwashers for Freeze-Distillation Desalination," *Desalination*, **4**, 5 (1968).

Barak, A., and G. Dagan, "An Analytical Investigation of the Flow in the Saturated Zone of Ice Counterwashers," *AIChE J.*, **16**, 10 (1970).

Kemp, N. H., "Analytical Solution of a Sink Model of a Two-Dimensional Counterwasher," *Desalination*, **12**, 127 (1973).

Probstein, R. F., and J. Shwartz, "Method of Separating Solid Particles from a Slurry with Wash Column Separators," *U.S. Patent No. 3,587,859* (June, 1971).

Shwartz, J., and R. F. Probstein, "Experimental Study of Slurry Separators for Use in Desalination," *Desalination*, **6**, 239 (1969).

Grossman, G., "Experimental Study of Pressurized Counterwasher for Freeze-Crystallization Desalination," *OSW Symposium on Freezing*, Boston, Mass. (Sept. 20-22, 1972). (Not published)

Bird, R. B., W. E. Stewart, and E. N. Lightfoot *Transport Phenomena*, pp. 411-412, Wiley, New York (1960).

Littman, H., R. G. Barile, and A. H. Pulsifer, "Gas-Particle Heat Transfer Coefficients in Packed Beds at Low Reynolds Numbers," *Ind. Eng. Chem. Fundamentals*, **7**, 554 (1968).

Eckert, E. R. C., *Heat and Mass Transfer*, pp. 199-200, McGraw Hill, New York (1959).

Manuscript received April 29, 1976; revision received August 3, and accepted August 9, 1976.

Simulation of an Electrochemical Carbon Dioxide Concentrator

The performance of an electrochemical device for the concentration of carbon dioxide from the atmosphere of a spacecraft cabin is analyzed. The removal rates as well as the concentration distributions of the different species are calculated for any set of operating conditions by a model which embodies the fundamental electrolyte properties and design parameters.

OMAR E. ABDEL-SALAM

and

JACK WINNICK

Chemical Engineering Department
University of Missouri-Columbia
Columbia, Missouri 65201

SCOPE

Electrochemical concentration emerged in the last few years as the best technique for carbon dioxide control in a long duration manned space flight (Winnick et al., 1974). There are two different designs under development for possible applications in a life-support system (Huddleston and Aylward, 1975; Woods et al., 1975). The former design has undergone several modifications in the past few years in order to improve its efficiency and widen its capability in various environment. First, a new electrolyte (tetramethylammonium carbonate) was introduced to replace cesium carbonate. Second, a new cathode with a relatively high porosity was found to improve the carbon dioxide removal rate to a great extent. Third, the matrix material and compression were changed in order to minimize the internal cell resistance and chemical deterioration in the electrolyte medium.

Preliminary experiments showed that these changes had a significant effect on the carbon dioxide removal rate. To obtain an optimum system design it was necessary to identify the factors which determine the carbon dioxide removal rate as well as the limits of cell operation. This was done through a model which simulates the fundamental transport processes taking place in the cell.

The carbon dioxide concentration is a multistep process involving mass transport in gas phases, chemical absorption and reaction in a liquid phase, and ionic transport in an electrolyte medium. The analysis of these processes (Lin and Winnick, 1974) yields two nonlinear ordinary differential equations which can be solved to obtain the carbon dioxide removal rate as well as the concentration distribution of the different species. This model was successfully used in simulating the performance of the early designs which used Cs_2CO_3 electrolyte.

Here we examine the applicability of this model in the present situation by utilizing the new electrolyte properties and the changes associated with the new cathode and matrix designs. The model is then used in the design of a full scale unit. In addition to operating

Correspondence concerning this paper should be addressed to Jack Winnick.

at the predetermined design conditions, the unit must be flexible enough to operate over a wide range of other operating conditions. This requires extrapolation of the known performance characteristics. The present model simulates the fundamental processes occurring in the cell, using, nearly exclusively, independently derived parameters. Predictions are therefore more reliable than those made strictly from empirical curve fitting.

The equations are of a general nature and can be used, with certain modifications, in the design of any electrochemical device which would remove and concentrate a pollutant from a gas or liquid stream.

CONCLUSIONS AND SIGNIFICANCE

The performance of a new electrochemical carbon dioxide concentrator can be simulated by a fundamental model embodying the electrochemical and physical properties of the electrolyte as well as parameters associated with the electrodes and electrolyte matrix. Two empirical assumptions are required; first, the rate constant of the CO_2-OH^- reaction is dependent on the square root of the hydroxyl ion concentration, and second, the active gas-electrolyte area is dependent on the current density. Both assumptions can be explained on physical grounds.

The experimental results obtained with a small scale cell were used to verify the model assumptions. From these results it was possible to design a full scale unit. The nominal current density chosen is a compromise between high current (carbon dioxide removal) efficiency and high carbon dioxide removal rates.

In addition to operation at the nominal conditions, the concentrator may also be required to work at other conditions. The model predicts the performance under these off-design conditions. The concentration distributions of the different species are also predicted. These determine the operating conditions which would lead to irreversible electrolyte precipitation.

The concept of electrochemical carbon dioxide concentration, originally developed for aircraft rebreather systems (Quattrone et al., 1970), has been found to meet all the requirements of establishing a long duration life-support system in a six-man spacecraft (Winnick et al., 1974). The process utilizes the hydrogen/oxygen fuel cell reaction to establish a hydroxyl ion concentration gradient between fuel-cell electrodes. Carbon dioxide is absorbed at the cathode and released at the anode. In this way the concentration of carbon dioxide in the cabin atmosphere is kept below a prescribed level. At the same time, the exhaled carbon dioxide is recovered in a concentrated form suitable for oxygen regeneration.

Crew activity (for example, maintenance) in remote regions of a spacecraft require a portable self-contained system designed specifically to be used by one man. One of the requirements imposed on such units is to have a capability of working over a wide range of air relative humidity, usually set between 35 and 90%. Therefore, the cell electrolyte is selected such that it remains soluble at the driest conditions at every point in the cell. Other provisions are also needed to accommodate the expected change in the electrolyte specific volume between the two extreme conditions.

The use of Cs_2CO_3 (Winnick et al., 1974) as the electrolyte is limited to air relative humidities above 60%. Lower humidities cause drying of the electrolyte leading to $CsHCO_3$ precipitation at the anode. This leads to hydrogen crossover to the air side, creating a hazardous situation. Precipitation of the electrolyte within the electrode pores can also decrease the active area available for the electrochemical reactions and will, correspondingly, result in the increase of the electrodes overvoltage. Humidity control of some sort can be used, but this adds to the total system equivalent weight which is of prime importance in space applications.

Two solutions for this problem have been proposed: the use of TMAC (tetramethylammonium carbonate) (Huddleston and Aylward, 1975) or the use of LSI-B* electrolyte (Woods et al., 1975). The saturated aqueous solutions of the carbonates and the bicarbonates of both electrolytes have much lower water vapor pressures than those of Cs_2CO_3 and $CsHCO_3$, enabling operation at lower air relative humidities. The expected change in the electrolyte specific volume between the two extremes of the air humidities is accommodated in the former design by the incorporation of a reservoir of porous Tissuquartz to adsorb the excess electrolyte at the humid conditions.† Controlled cell cooling and careful selection of the electrode to matrix volume is the method used in the latter design.

Among other modifications in this design, new electrodes and new cell matrix material and compression have been used to improve carbon dioxide removal rates and power efficiency.

Optimum design of the concentrator requires an accurate model which can simulate the cell performance over a wide range of operating conditions. Knowledge of the concentration distribution of the different species is needed to predict the incidence of precipitation in low humidity environments. These concentrations may also be useful in determining the IR drop and overvoltage components in the cell. The determination of these concentrations in an actual operating cell is experimentally difficult because of the small thickness of the cell.

We will present a model which simulates the performance of this new cell design (Huddleston and Aylward, 1975) using basic physicochemical data. No attempt is made here to analyze the performance of the latter design (Woods et al., 1975) because of the lack of properties of the proprietary electrolyte (LSI-B). When these properties become available, the model can be used with this design.

THEORY

The mechanisms of cell reactions in the carbon dioxide concentrator have been described in a previous work (Winnick et al., 1974). Basically, they are:

* A proprietary electrolyte of Life Systems, Inc., Cleveland, Ohio.

† Recent results from full scale tests (Huddleston and Aylward, 1975) indicate that a cell of this design charged with a single concentration of TMAC is not capable of operation over the entire proposed range of 35 to 90%. The variation in the electrolyte specific volume is not quite compensated by the inclusion of a reservoir into the cell. Improvements in the mechanical design would be required to enable coverage of the entire range.

1. The cathode reactions leading to the carbonate formation from the absorbed carbon dioxide:

$$1/2\ O_2 + H_2O + 2e^- \rightarrow 2OH^- \quad (1)$$

$$CO_2 + OH^- \rightarrow HCO_3^- \quad (2)$$

$$HCO_3^- + OH^- \rightleftarrows CO_3^{2-} + H_2O \quad (3)$$

2. The conversion of the carbonate ions to bicarbonate ions by reaction (3) as they move from a high pH at the cathode to a low pH at the anode.

3. The decomposition of the bicarbonate ions releasing carbon dioxide at the anode

$$HCO_3^- \rightarrow CO_2 + OH^- \quad (4)$$

$$HCO_3^- + H_2O \rightarrow H_2CO_3 + OH^- \quad (5)$$

$$H_2CO_3 \rightarrow CO_2 + H_2O \quad (6)$$

4. The formation of water at the anode

$$H_2 \rightarrow 2H^+ + 2e^- \quad (7)$$

$$2H^+ + 2OH^- \rightarrow 2H_2O \quad (8)$$

If the carbonate ions were the only charge carriers in the solution, then 1 mole of carbon dioxide would be transferred for each two Faradays of electric current. This corresponds to 100% current efficiency. In practice, some of the hydroxyl ions escape from the cathode region without reaction with carbon dioxide or HCO_3^- ions, reacting with the H^+ ions at the anode to form water. This leads to a lower current efficiency.

The analysis of the transport equations (Appendix A) depends on dividing the cell into subcells in the direction of the air flow and subdividing each subcell into five zones as shown in Figure 1. The analysis leads to the following two nonlinear ordinary differential equations:

$$f_1(C_1, C_3)\frac{dC_1}{dx} + f_2(C_1, C_3)\frac{dC_3}{dx} = -N_{5T} + f_3(C_1, C_3)I/F \quad (9)$$

$$f_4(C_1, C_3)\frac{dC_1}{dx} + f_5(C_1, C_3)\frac{dC_3}{dx} = -I/F + f_6(C_1, C_3)I/F \quad (10)$$

The boundary condition at the cathode is

$$N_{5T} = S_c(k_i D_{5c} C_2)^{1/2}[C_{5c} - C_1/(K_i C_2)] \quad \text{at} \quad x = -d/2 \quad (11)$$

where

$$C_{5c} = \{(P_{5c})_I - N_{5T}ART/[V_c(1 - \exp\{-h_{5c}A/V_c\})]\}/E \quad (12)$$

The boundary condition at the anode is similar except that k_i is replaced by $(k_i + k'_{iii}a_6)$ and the subscript c by a. The third boundary condition is obtained from the energy and water balance equations (Lin et al., 1974). It arises from the condition, at steady state, that all water produced at the anode must be released at the cathode. The anode gas flow rate is too low to remove a significant amount of water. This boundary condition is

$$C_1 + C_3/(C_1K_{ii}) + 2C_3 = C_4 = f(P^*_{6c}, T_c) \quad \text{at} \quad x = -d/2 \quad (13)$$

These equations contain several parameters depending on solution properties, electrode design, and matrix material and compression. To obtain the parameters related to cell design, a small scale cell was constructed and tested with TMAC. Fundamental property tests were also made to obtain the electrolyte properties and the effect of the matrix compression on the internal cell resistance.

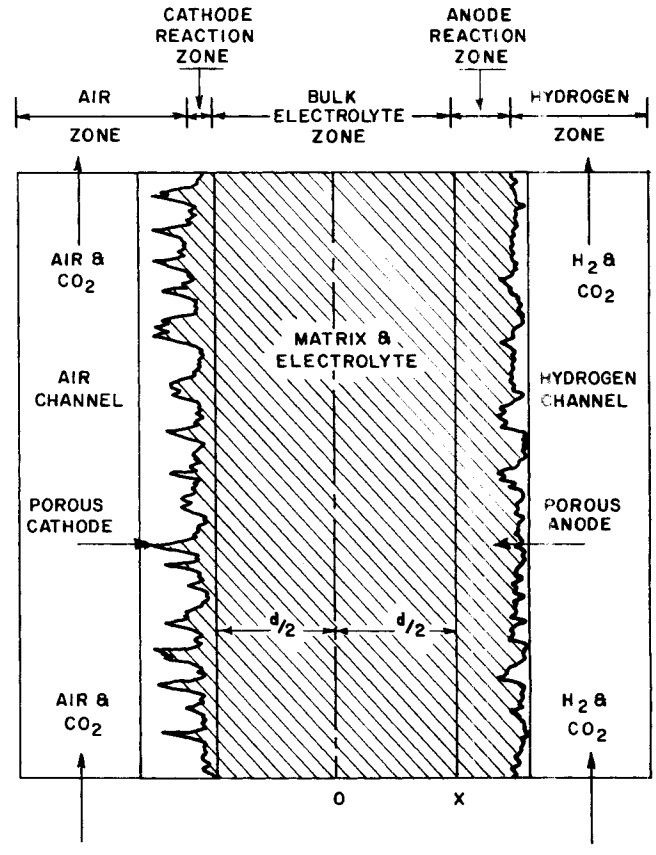

Fig. 1. Schematic of subcell.

ANALYTICAL CELL DESIGN

The analytical cell was constructed of one layer of Tissuquartz of 0.46 mm (18 mils) thickness sandwiched between two layers of fuel-cell asbestos, 0.51 mm (20 mils) each, and the whole compressed to a final thickness of 0.64 mm (25 mils). The electrodes were made of metallic screens upon which a mixture of platinum and teflon was applied. The electrode length in the air flow direction was 152.4 mm (6 in.), and the width was 25.4 mm (1 in.). Previous experience showed that increasing the cathode porosity had a favorable effect on the carbon dioxide removal rate; the later cathode designs have reflected this observation. The anode material and catalyst loading were chosen so as to minimize the anode overvoltage. The whole system was enclosed in a metallic housing with four rectangular air ducts, 5.1 × 4.8 mm (0.2 × 0.19 in.) each.

ANALYTICAL CELL TESTS

The carbon dioxide removal rate was measured at selected conditions of current densities between 12.9 and 32.3 mA/cm² (12 to 30 A/ft²), P_{CO_2} in the range 0.25 to 4 mm Hg, air velocities in the range 151 to 463 cm/s (5 to 15 ft/s), air temperature of 21.1°C, and air relative humidities in the range 34 to 71%. The hydrogen flow rate was fixed at about 10 cm³/s. Each test was run for approximately 2 days with at least three data readings taken each day. The results of these tests were reported by Huddleston and Aylward (1973). Generally, the reported data were accurate to ± 4%.

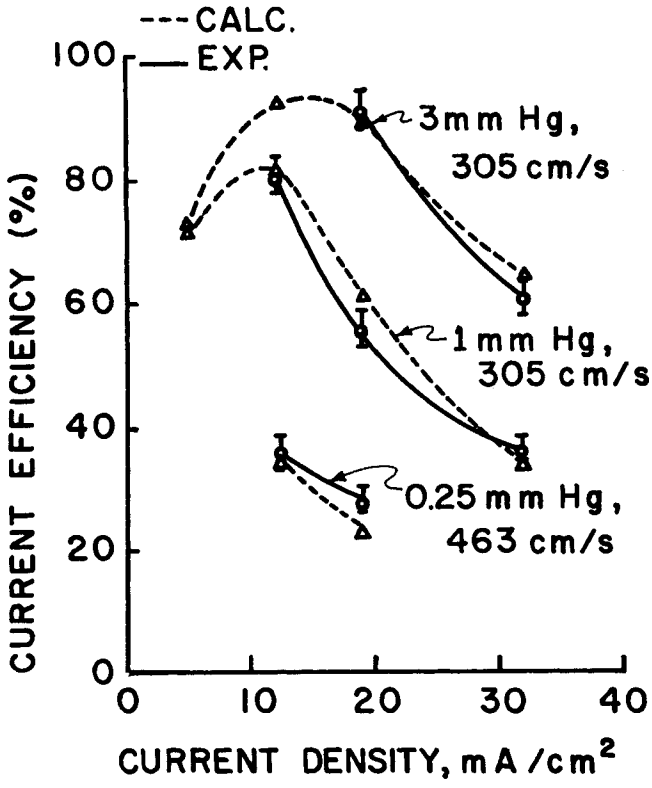

Fig. 2. Current (carbon dioxide removal) efficiency in the analytical cell.

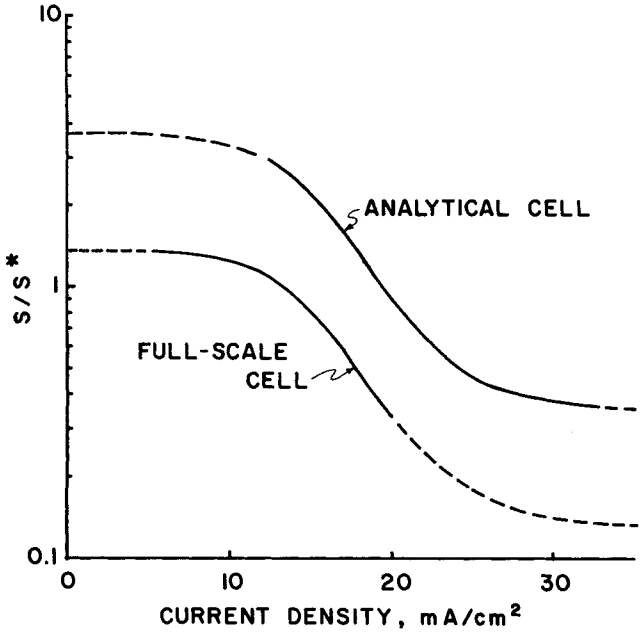

Fig. 3. Effect of current density on active cathode area. (S* is S for analytical cell at $I = 19.3$ mA/cm^2).

PARAMETER EVALUATION

Electrolyte Parameters

The electrolyte parameters including the activity coefficients, diffusion coefficients, and mobilities were calculated from the water vapor pressure data, viscosities, densities, and specific conductivities of $(NMe_4)_2CO_3$, NMe_4HCO_3, and NMe_4OH solutions (Aylward, 1974). The detailed calculations and tables are available elsewhere (Abdel-Salam, 1976).

Henry's Law Constants

No data were available for the physical solubility of carbon dioxide in aqueous $(NMe_4)_2CO_3$ and NMe_4HCO_3 solutions. The Henry's law constants are different from their values at infinite dilution by a factor depending on the activity coefficients of carbon dioxide in the solution. A theoretical expression due to Van Krevelen and Hoftijzer (1948) represents this relation as follows:

$$\log (H/H^o) = (i_+ + i_- + i_g)\mu \qquad (14)$$

This expression was used by taking i_+ as 0.030, i_- as 0.021, and i_g as -0.010. The value of i_+ is the reported value for NH_4^+ ion, since there was no value reported for NMe_4^+ ion. This may result in some error in estimating H, but this will not have a significant effect on the calculations since H appears in the analysis only in conjunction with the empirically determined cathode active area. The values used for i_- and i_g are those of CO_3^{2-} and carbon dioxide, respectively.

Carbon Dioxide Diffusivity in the Solution

The molecular diffusivity of carbon dioxide in the solution was estimated from the following formula obtained for carbon dioxide diffusion in viscous liquids (McManamey and Woollen, 1973):

$$D = D^o\,(\eta/\eta^o)^{0.47} \qquad (15)$$

Gas-Phase Mass Transfer Coefficients

The data obtained in the analytical cell at a current density of 19.3 mA/cm^2 and air velocity of 305 cm/s were used to estimate the gas-phase mass transfer coefficient for carbon dioxide in the air zone. At a low P_{CO_2}, the process becomes gas-phase mass transfer controlled, and in the limit of zero P_{CO_2} Equation (12) reduces to

$$h_{5c} = -\,(V_c/A)\,\ln\left[1 - (ART/V_c)\left(\frac{dN_{5T}}{dP_{5c}}\right)_{P_{5c}=0}\right] \qquad (16)$$

The calculated mass transfer coefficient was 6% lower than that for laminar flow in rectangular ducts with uniform wall concentration (Knudsen and Katz, 1958):

$$Sh = Sh_\infty\,[1 + (0.003 + 0.039\,s_1/s_2)\,Re\,Sc\,d_e/L] \qquad (17)$$

It was assumed that for air velocities normally used in the cell, the gas-phase mass transfer coefficients of carbon dioxide are always 94% of that calculated from the above expression. Other mass transfer coefficients (for example, that of water vapor in the air stream) were estimated from similar expressions (Abdel-Salam, 1976). The heat transfer coefficients were estimated from a slightly different expression for heat transfer in rectangular ducts with uniform heat flux (Knudsen and Katz, 1958):

$$Nu = Nu_\infty[1 + (0.003 + 0.019\,s_1/s_2)\,Re\,Pr\,d_e/L] \qquad (18)$$

Matrix Labyrinth Factor

To calculate the effective diffusion coefficients and mobilities in the matrix zone, the values in free electrolytes should be multiplied by a factor depending on the matrix material and compression. This factor was determined independently by comparing the electrical resistance of one free electrolyte with that of the matrix-electrolyte combination in a special micrometer cell (Huddleston and Aylward, 1973). The matrix labyrinth factor at the same compression used in the cell was 0.34.

Gas-Electrolyte Interface Area in the Anode

Experimental as well as simulation results show that the carbon dioxide removal rate is almost independent of the anode parameters. Therefore, an approximate value of the parameter $S_a[D_5(k_i\ C_2 + k'_{iii}\ a_6)]^{1/2}$ which appears in Equation (11) when written for the anode zone, was estimated from test data and the approximate compositions expected in the cell. This parameter was then used as such in the model.

Gas-Electrolyte Interface Area in the Cathode

Experimental as well as simulation results show that the carbon dioxide removal rate is highly dependent on the cathode parameters. The air-catholyte interface area can be selected so that the calculated carbon dioxide removal rates match the experimental results. Calculations show that the test data (Figure 2) can be simulated within experimental error only if the rate constant k_i was proportional to $C_2^{1/2}$ and if the air-catholyte area is presumed dependent upon the current density as shown in Figure 3. The calculated current efficiencies are represented by the dotted lines in Figure 2. The dependence of the reaction rate constant on the square root of the hydroxyl ion concentration and the gas-electrolyte interface area on the current density is explained in Appendix B. The calculated results are in good agreement with the experimental data. The effect of P_{CO_2} on the carbon dioxide removal efficiency is correctly predicted by the model.

The model predicts optimum current densities, resulting in maximum current efficiencies, which vary with P_{CO_2}. The presence of an optimum current density for each value of P_{CO_2} has been previously reported for similar devices (Marshall et al., 1973). However, the present model predicts these extrema from fundamental considerations.

No significant effect of the cell temperature, hydrogen flow rate, or hydrogen-anolyte interface area is seen on the carbon dioxide removal efficiency. On the other hand, this efficiency is greatly dependent on the air-catholyte interface area.

FULL SCALE CELL DESIGN

The NASA one-man unit standard for carbon dioxide production is 1 kg/man day. To maintain the manned spacecraft within the prescribed limits, the life support system must remove the carbon dioxide at this same rate from the ambient condition of 3 mm Hg partial pressure and air relative humidities between 35 and 90%. The unit can be used for ambient carbon dioxide concentrations up to 15 mm Hg, but if the concentration in the cabin atmosphere exceeds that limit, the unit is shut down and other systems (for example, LiOH absorbers) are used to resume the normal concentration in a short period after which the system is started again. It is possible by using the same device to reduce the carbon dioxide concentration in the cabin atmosphere to earthlike conditions (0.25 mm Hg), but this would require three to four times more cells.

Since operation will occur mainly at the nominal conditions, a primary design consideration is achievement of high current (carbon dioxide removal) efficiency at these conditions. Figure 2 shows that the model predicts a maximum efficiency at 3 mm Hg carbon dioxide partial pressure at a current density of about 15 mA/cm^2. These same results, plotted instead as actual carbon dioxide removal flux vs. current density (Figure 4), show a relatively large slope at this point. This means that increasing the current density slightly from the value at the maximum efficiency greatly lowers the transfer area needed. A compromise design was arrived at, 2940 cm^2, requiring 19.3 mA/cm^2 (18 A/ft^2) at nominal conditions.

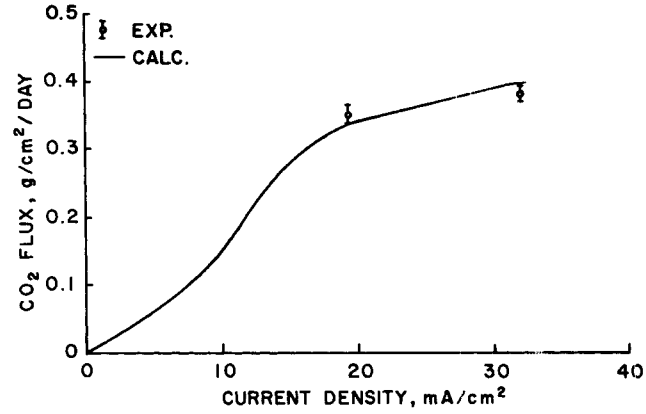

Fig. 4. Carbon dioxide removal rates in the analytical cell at an air inlet P_{CO_2} of 3 mm Hg.

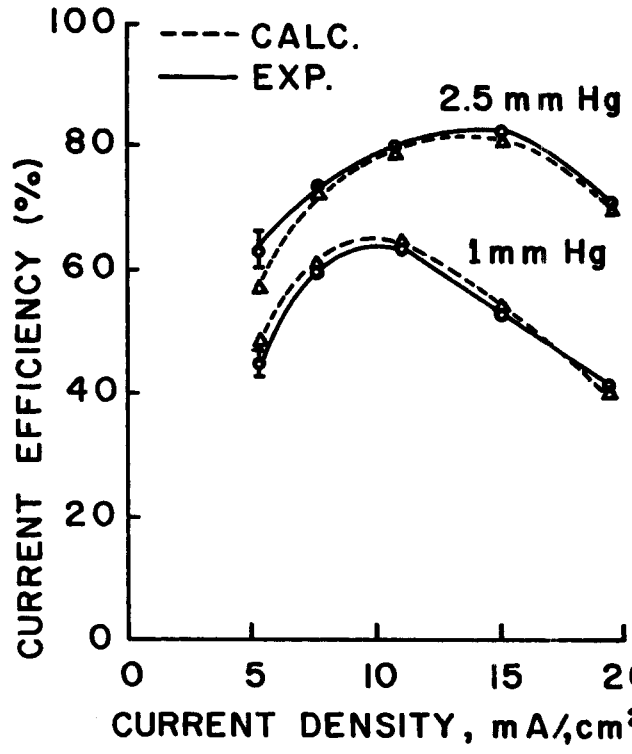

Fig. 5. Current (carbon dioxide removal) efficiency in the full scale cell.

Previous experience of using analytical cell data in full scale cell sizing showed that a safety factor of about 20 to 30% in electrode area may be required. Accordingly, a full scale (one-man) system was fabricated consisting of four identical cell pairs with common hydrogen chambers to give a total electrode area of 3 720 cm^2 (4 ft^2). Each cell was made of the same fuel-cell hardware used in the analytical cell, except that the width of each electrode was twelve times that used in the analytical cell (305 mm, or 12 in.); that is, there were forty-eight air ducts per electrode instead of four. The air path length was kept the same as in the analytical cell (152.4 mm, or 6 in.).

FULL SCALE CELL TESTS

Parametric testing results were obtained for current densities of 5.4 to 19.3 mA/cm^2 (5 to 18 A/ft^2) and P_{CO_2} of 1 and 2.5 mm Hg. The air velocity was fixed at 203 cm/s (6.6 ft/s). No other variation of test conditions was made except for the decrease of the inlet air relative humidity from 71 to 34% in the last stages of the program.

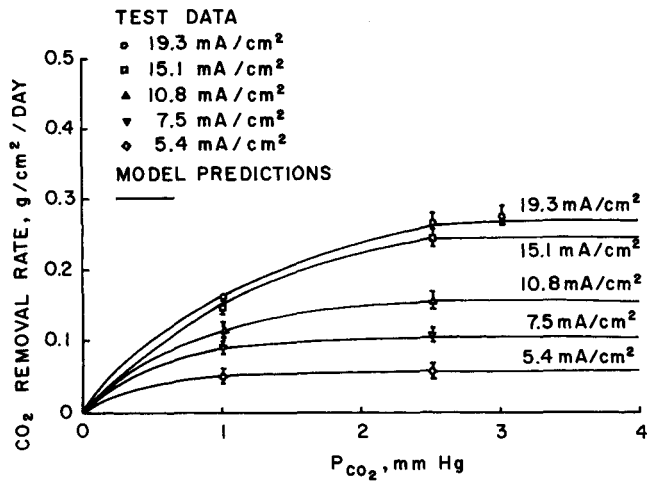

Fig. 6. Model predictions of carbon dioxide removal rates in the full scale cell.

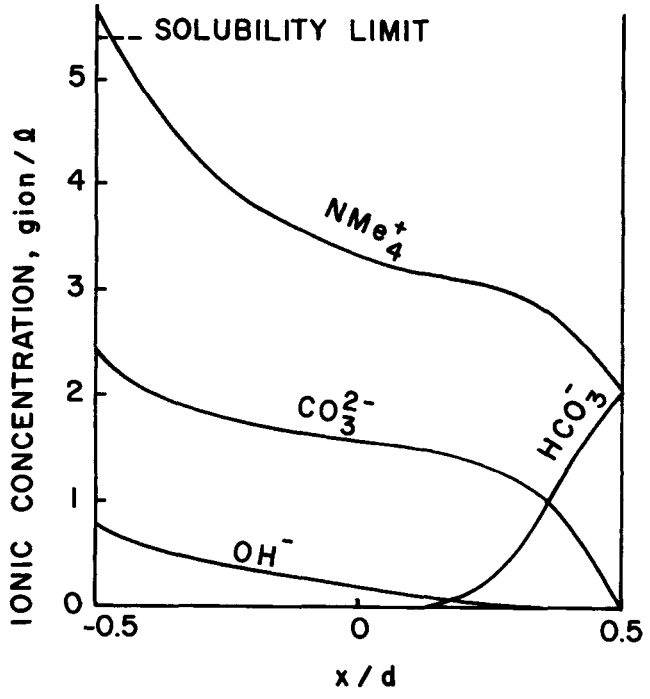

Fig. 7. Predicted ionic concentration distribution in the analytical cell at the following conditions: P_{CO_2} = 4 mm Hg, I = 32.9 mA/cm², air velocity = 203 cm/s, air temp. = 21.1°C, air dew point = 4.4°C, cell voltage = 0.3V.

The results of these tests were summarized by Huddleston and Aylward (1975). The current efficiencies were, as expected, lower than those of the analytical cell at the same test conditions. They are shown in Figure 5. Since there was no difference between the full scale and analytical cell designs except in the dimensions of the electrodes, this reduction in the carbon dioxide removal is probably due to the decrease in the specific cathode active area. By using a constant scaling-down factor of 0.37 for the active area as shown in Figure 3, the full scale cell data were simulated (Figure 5).

MODEL PREDICTIONS

Effect of P_{CO_2}

At a constant current density, increasing P_{CO_2} in the inlet cabin air increases the carbon dioxide removal rate. This is apparent from Figure 6 which gives model predictions at off-design conditions. The increase is rather sharp in the low P_{CO_2} region, becoming much slower as P_{CO_2} exceeds the base line condition (3 mm Hg).

The increase in P_{CO_2} in the air zone reduces the OH^- concentration in the catholyte as predicted by the model. This is in agreement with the pH measurements of the catholyte in the analytical cell (Huddleston and Aylward, 1973). This also explains the increase of the cathode overvoltage with P_{CO_2} increase (Huddleston and Aylward, 1973).

Effect of Current Density

The simulated results as well as the experimental data show that there is a maximum current efficiency at a certain current density for each value of P_{CO_2}, and the value of the optimum current density increases with P_{CO_2}. It is necessary to operate at or near this current density in order to obtain best utilization of consumables (hydrogen and oxygen). The existence of an optimum current efficiency is associated with a certain OH^- concentration in the catholyte at which carbon dioxide removal efficiency is maximum. The optimum OH^- concentration is dependent on the carbon dioxide concentration at the air inlet.

Effect of Air Velocity

In the experimental air velocity range (151 to 463 cm/s), actual as well as model results show little effect on the carbon dioxide removal rate at the design P_{CO_2} concentration (3 mm Hg) and above. The carbon dioxide removal rate decreases gradually as the velocity decreases below that level, indicating the influence of gas-phase mass transfer limitations. In the low P_{CO_2} region ($\leq$ 0.25 mm Hg), the process becomes totally controlled by the gas-phase mass transfer coefficient. In that range the increase of the carbon dioxide flux with air velocity is accompanied by a decrease in the OH^- concentration which also increases the cathode overvoltage, verified experimentally. As the P_{CO_2} increases above this level, the effect of the air velocity diminishes.

Effect of Matrix Thickness and Compression

The matrix thickness and compression are chosen on the basis of the internal cell resistance and other mechanical considerations. However, it is desirable to predict the effect on the carbon dioxide removal rate of changing these parameters. Increasing the matrix thickness from the design value over a small range causes a predicted increase in the carbon dioxide removal rate. This increase is due to the decrease in HCO_3^- ion back diffusion from anode to cathode. The carbon dioxide removal efficiency reaches a maximum, then decreases again as the matrix thickness increases. This decrease is due to the increase of the OH^- flux from cathode to anode to maintain the constancy of the cell current, which decreases the carbon dioxide removal efficiency. The effect of the matrix thickness on the carbon dioxide removal rate as predicted by the model agrees completely with prior experiments on similar systems (Marshall et al., 1973).

Increase of the cell compression over a limited range, simulated in the model by use of a lower matrix labyrinth factor, also increases the carbon dioxide removal rate. This is due to effects similar to those involved in increasing the thickness. The total effect on the internal cell resistance must be considered in obtaining the optimum thickness and compression for certain design conditions.

Effect of Air Relative Humidity and Temperature

Solubility Limitations. The model is important in predicting the limits of cell operation in low humidity environments. Unlike $CsHCO_3$, the molar solubility of NMe_4HCO_3 is high enough (7.3 g mole/l at room temperature) to avoid precipitation of the electrolyte at the anode. On the other hand, the solubility of $(NMe_4)_2CO_3$ is low (2.7

g mole/l at room temperature), and it can precipitate when the concentration of the catholyte in equilibrium with the air humidity condition exceeds the solubility limits. Figure 7 shows the concentration distribution of the different species in one case at which precipitation is predicted at the cathode. The concentration of the catholyte is considered to be the total cation concentration, and precipitation is indicated if it exceeds 5.4 g ion/l.

The humidity-current density criteria in the TMAC units are different from those in the Cs_2CO_3 units (Lin et al., 1974). Since $CsHCO_3$ precipitation is the limiting factor in the case of Cs_2CO_3 units, precipitation is indicated when the current density drops below a certain value for a fixed air humidity condition. This reduces the cation concentration gradient across the matrix and increases the $CsHCO_3$ concentration at the anode. On the other hand, precipitation of the catholyte in the TMAC units is determined by several factors, including current density, cell voltage, and air humidity. These are discussed below. The energy and water balance lead to the following two equations (Lin et al., 1974):

$$T_c = (T)_I - I(\Delta H_R/2F + E/J)$$
$$\{Z/(\rho V c_P L) + 1/[2\,U_c n(s_1 + s_2)L]\} \quad (19)$$

$$(P_{6c})_O = (P_{6c})_I + IRT/(2h_{6c}F) \quad (20)$$

From these equations together with the water vapor pressure data of $(NMe_4)_2CO_3$ solutions, Table 1 was constructed to show the limit of the full scale cell operation at an air relative humidity of 33.6%, assuming a fixed cell potential of 0.2 V. The probable small increase in $(NMe_4)_2CO_3$ solubility with temperature was ignored. Unlike the Cs_2CO_3 cells, incidence of precipitation with TMAC increases with current density.

We have no precise experimental verification of the predicted concentrations. As part of the experimental program, however, rough *p*H measurements were made of the catholyte and anolyte from *p*H paper. Table 2 contains the calculated and experimental *p*H values obtained in the analytical cell at a current density of 19.3 mA/cm² and an air inlet relative humidity of 71.2%. The calculated *p*H values were obtained by assigning an activity coefficient of unity for the OH^-. The true individual ionic activity coefficient cannot be determined or estimated without a nonthermodynamic assumption. The measured values will also contain some error (about ± 0.5), not only because of the approximate nature of the *p*H papers used, but also because the taking of representative samples of surface catholyte or anolyte is difficult. The direction of deviation of the measurements from the predictions confirms this suggestion.

Carbon dioxide transfer efficiency. The model predicts a 6% increase in the carbon dioxide removal efficiency of the analytical cell operating at 3 mm Hg P_{CO_2} and 19.3 mA/cm² as the air relative humidity decreases from 71 to 34%. The earliest data obtained with the analytical cell did not show a significant effect of this parameter beyond the experimental error limits (Huddleston and Aylward, 1973). Later data on the full scale cell (Huddleston and Aylward, 1975) in the very low humidity region (15 to 20%) agree qualitatively with the results of the model. Precipitation is predicted at these low humidities; however, it has been reported that TMAC can form unstable supersaturated solutions (Huddleston and Aylward, 1972).

The increase of the carbon dioxide removal rate predicted by the model is due to the increase of electrolyte viscosity with concentration which increases the selectivity of CO_3^{2-} ions as charge carriers and increases the carbon dioxide removal rate. This viscosity increase will be more marked at the very low humidities (high TMAC concentrations).

Changing the temperature over a limited range has little effect on the carbon dioxide removal rates because the increase in the reaction rate constant k_i with temperature compensates for the decrease in the electrolyte viscosity.

Table 1. Precipitation Predictions in the Full Scale Cell at an Air Inlet Temperature of 21.1°C, Air Dew of 4.4°C, and Air Velocity of 203 cm/

Current density, mA/cm²	Average cell temperature, °C	Average water partial pressure, mm Hg	Catholyte concentration, g ion/l
5	22.4	6.37	5.23 (no precipitation)
10	23.8	6.44	5.29 (no precipitation)
15	25.1	6.51	5.36 (no precipitation)
20	26.4	6.58	5.43 (precipitation)
25	27.7	6.65	5.48 (precipitation)
30	29.1	6.72	5.61 (precipitation)

Table 2. Predicted and Measured *p*H Values in the Analytical Cell at a Current Density of 19.3 mA/cm² and Air Relative Humidity of 71.2%

Inlet P_{CO_2}, mm Hg	Catholyte *p*H		Anolyte *p*H	
	Measured	Predicted	Measured	Predicted
0.25	13.5	14.3	9.2	8.1
1	13.3	14.1	9.2	8.4
4	13.0	13.4	9.0	8.7

Effect of Hydrogen Flow Rate and Gas-Anolyte Interface Area

As mentioned earlier, conditions at the anode have little effect on the calculated carbon dioxide flux. The only conclusion that can be obtained from the model is that decreasing these parameters lowers the anolyte *p*H which increases the anode overvoltage (Huddleston and Aylward, 1973) probably by the formation of an adsorbed carbon dioxide complex layer on the anode or by increasing the sticking of the matrix to the anode surface.

CONCLUSIONS

The study showed that the performance of the carbon dioxide concentrator using TMAC can be simulated by a fundamental model of the mass transfer and reaction rates of the processes which take place in the cell. Most of the model parameters have been estimated from independent measurements. The only assumptions required to simulate test data were the dependence of the rate constant of the carbon dioxide-OH^- reaction on the square root of the OH^- concentration and the dependence of the air-catholyte interface area on the current density. The model enabled the design and simulation of a full scale cell over a wide range of operating conditions. The concentration distribution of the different species were also calculated.

ACKNOWLEDGMENT

Financial support for this work was provided from a grant by the NASA Johnson Space Center, Houston, Texas.

NOTATION

a = activity
A = geometric electrode area
c_p = specific heat of air

C = molar concentration
d = matrix thickness
d_e = equivalent diameter of rectangular channel
D = molecular diffusivity or ionic diffusion coefficient
E = cell voltage
$f_1, f_2, f_3, f_4, f_5, f_6$ = functions of concentrations, diffusion coefficients, mobilities, and equilibrium constants defined by Equations (A6) to (A12)
F = Faraday's constant
h = gas-phase mass transfer coefficient
H = Henry's law constant
ΔH_R = heat of formation of water vapor
i = coefficient defined by Equation (14)
I = current density
J = mechanical heat equivalent
k = reaction rate constant
K = reaction equilibrium constant
L = length of air channel
n = number of air channels per electrode
N = molar flux
Nu = Nusselt number
P = pressure
Pr = Prandtl number
R = universal gas constant
Re = Reynolds number
s_1 = length of short side of rectangular duct
s_2 = length of long side of rectangular duct
S = gas-electrolyte interface area per unit of geometric electrode area
Sc = Schmidt number
Sh = Sherwood number
T = air temperature
T_c = cell temperature
u = ionic mobility
U = gas-phase heat transfer coefficient
v = solution bulk velocity
V = volumetric gas flow rate
x = coordinate dimension between electrodes
z = ionic charge
Z = coordinate dimension in the air flow direction

Greek Letters

γ = activity coefficient
η = viscosity
μ = ionic strength
ρ = air density
ϕ = electrical potential
ψ = function defined by Equation (A12)

Subscripts

a = anode
c = cathode
g = gas
I = inlet
O = outlet
T = total
1 = HCO_3^-
2 = OH^-
3 = CO_3^{2-}
4 = NMe_4^+
5 = carbon dioxide
6 = water
i = reaction (2)
ii = reaction (3)
iii = reaction (6)
$+$ = cation
$-$ = anion
∞ = limiting value
$\dagger$ = activated complex

Superscripts

$*$ = interfacial value
o = infinite dilution
$'$ = backward reaction

APPENDIX A: FUNDAMENTAL EQUATIONS

The following treatment is slightly different from the analysis given by Lin and Winnick (1974). The mass transfer in the gas phase is represented by the equation

$$N = h(P - P^*)_{l.m.}/RT \tag{A1}$$

The reaction between carbon dioxide and OH^- results in the following equation:

$$N = (k_i D_5 C_2)^{1/2}[(P^*/H) - C_1/(K_i C_2)]S_c \tag{A2}$$

The second term inside the brackets is much smaller than the first term at the cathode under normal operation and can be neglected. The combination of Equations (A1) and (A2) results in the boundary condition (11). Similar treatment gives the boundary condition at the anode.

The ionic transport in the electrolyte is represented by the Nernst-Planck equation:

$$N_j = -\left(D_j \frac{dC_j}{dx} + z_j F u_j C_j \frac{d\phi}{dx} \right) + C_j v \tag{A3}$$

In the concentrator, almost all the water produced at the anode is removed by the air stream. The bulk velocity term is approximately calculated from the water transport in the cell. However, the assumption of zero bulk velocity (Lin and Winnick, 1974) does not cause a significant change in results. The following equations result from the conservation of mass and charge at steady state:

$$N_1 + N_3 + N_5 = N_T \tag{A4}$$

$$N_1 + N_2 + 2N_3 = I/F \tag{A5}$$

By substituting for each term from Equation (A3) and utilizing the reaction equilibrium relations and electroneutrality, we obtain Equations (7) and (8) where

$$f_1 = D_1 + D_4(C_1^2 - C_3/K_{ii})(u_1 + 2u_3C_3/C_1)/(u_4\psi) + 2D_5K_{ii}C_1/(K_iC_3) \tag{A6}$$

$$f_2 = D_4(2C_1 + 1/K_{ii})(u_1C_1 + 2u_3C_3)/(u_4\psi) + D_3 - D_5K_{ii}C_1^2/(K_iC_3^2) \tag{A7}$$

$$f_3 = (C_1 + C_3 + C_5 - C_1u_1/u_4 - 2C_3u_3/u_4)/(2C_T) \tag{A8}$$

$$f_4 = D_1 + D_4(C_1^2 - C_3/K_{ii})\,[u_1 + u_2C_3/(K_{ii}C_1^2) + 4u_3C_3C_1]/(u_4\psi) - D_2C_3/(K_{ii}C_1^2) \tag{A9}$$

$$f_5 = D_4(2C_1 + 1/K_{ii})\,[u_1C_1 + u_2C_3/(K_{ii}C_1) + 4u_3C_3]/(u_4\psi) + 2D_3 + D_2/(K_{ii}C_1) \tag{A10}$$

$$f_6 = (C_1 + C_2 + 2C_3 - C_1u_1/u_4 - C_2u_2/u_4 - 4C_3u_3/u_4)/(2C_T) \tag{A11}$$

and ψ is given by

$$\psi = C_1^2 + 2C_1C_3 + C_3/K_{ii} \tag{A12}$$

APPENDIX B: MODEL JUSTIFICATION

The dependence of the reaction rate constant k_i on the square root of the hydroxyl ion concentration in the catholyte requires some justification. The reaction rate constant in concentrated solutions is different from the value at infinite dilution by a factor depending on the activity coefficients of carbon dioxide, OH^- ions, and the activated complex formed during the absorption reaction (Frost and Pearson, 1961). The following equation represents this relation:

$$\log k = \log k^o + \log(\gamma_{CO_2} + \gamma_{OH^-} - \gamma_\dagger) \tag{B1}$$

The rapidly increasing activity coefficients of NMe_4OH with concentration (Abdel-Salam et al., 1976) suggest that the reaction rate constant depends, in some way, on the OH^- concentration. Further support of that view comes from the early work on the alkaline decomposition of diacetone alcohol in presence of NMe_4OH and KOH, successively (Halberstadt and Prue, 1952). The reaction rate in that case increased with increasing NMe_4OH concentration but decreased slightly in the case of KOH. This behavior is consistent with the activity coefficients of the two electrolytes.

The dependence of the gas-catholyte interface area on the current density and the electrode configuration is less clearly understood. It is known that the equilibrium of the electrolyte meniscus inside the electrode pores depends on several factors, such as the capillary forces, gas pressure, etc. It may be that the electroosmotic forces, which depend on the current density distribution in the electrode, affect the air-electrolyte equilibrium and hence their interface area.

LITERATURE CITED

Abdel-Salam, O. E., J. E. Bauman, Jr., and J. Winnick, "Activity Coefficients of some Tetramethylammonium Electrolytes," *J. Phys. Chem.*, submitted for publication (1976).

Adel-Salam, O. E., "Simulation of Carbon Dioxide Concentrator," Ph.D. dissertation, Univ. Mo., Columbia (1976).

Aylward, J. R., "Hydrogen Depolarized Carbon Dioxide Concentrator Electrochemical Cell Electrolyte Properties," Intermediate Report, Contract NAS 9-13679, National Aeronautics and Space Administration, Johnson Space Center, Houston, Tex. (Dec., 1974).

Frost, A. A., and R. G. Pearson, *Kinetics and Mechanism: A Study of Homogeneous Chemical Reactions*, 2nd ed., pp. 150-152, Wiley, New York-London (1961).

Halberstadt, E. S., and J. E. Prue, "Kinetic Salt Effects on the Decomposition of Diacetone Alcohol in Solutions of Tetraalkylammonium Hydroxides," *J. Chem. Soc.*, 2234 (1952).

Huddleston, J. C., and J. R. Aylward, "Development of An Integrated Water Vapor Electrolysis Oxygen Generator and Hydrogen Depolarized Carbon Dioxide Concentrator," Intermediate Report, Contract NAS 9-11830, National Aeronautics and Space Administration, Manned Space Center, Houston, Tex. (May, 1972).

———, "Hydrogen Depolarized Carbon Dioxide Concentrator Performance Improvements and Cell Pair Structural Tests," Intermediate Report, Contract NAS 9-12920, National Aeronautics and Space Administration, Johnson Space Center, Houston, Tex. (Sept., 1973).

———, "One-Man Electrochemical Air Revitalization System," Final Report, Contract NAS 9-13679, National Aeronautics and Space Administration, Johnson Space Center, Houston, Tex. (May, 1975).

Knudsen, T. G., and D. L. Katz, *Fluid Dynamics and Heat Transfer*, p. 338, McGraw-Hill, New York (1958).

Lin, C. H., and J. Winnick, "An Electrochemical Device for Carbon Dioxide Concentration II. Steady State Analysis CO_2 Transfer," *Ind. Eng. Chem. Process Design Develop.*, 13, 63 (1974).

Lin, C. H., M. L. Heinemann, and R. M. Angus, "An Electrochemical Device for Carbon Dioxide Concentration III. Steady State Analysis-Energy and Water Transfer," *ibid.*, 13, 261 (1974).

Marshall, R. D., F. H. Schubert, and J. N. Carlson, "Electrochemical Carbon Dioxide Concentrator: Math Model," Final Report, Contract NAS 2-6478, National Aeronautics and Space Administration, Ames Research Center, Moffett Field, Ca. (Aug., 1973).

McManamey, W. J., and J. M. Woollen, "The Diffusivity of Carbon Dioxide in Some Organic Liquids at 25°C and 50°C," *AIChE J.*, 19, 667 (1973).

Quattrone, P. D., A. D. Babinski, and R. A. Wynveen, "Carbon Dioxide Control and Oxygen Generation," ASME Paper No. 70-AV/SpT-8, Los Angeles Meeting, Calif. (June, 1970).

Van Krevelen, D. W., and P. J. Hoftijzer, "Sur la Solubilite des Gas dans les Solutions Aqueuses," *Chim. Ind. XXI mme Congres Int. Chim. Ind.*, 168 (1948).

Winnick, J., R. D. Marshall, and F. H. Schubert, "An Electrochemical Device for Carbon Dioxide Concentration I. System Design and Performance," *Ind. Eng. Chem. Process Design Develop.*, 31, 59 (1974).

Woods, R. R., F. H. Schubert, and T. M. Hallick, "Electrochemical Air Revitalization System Optimization Investigation," Final Report, Contract NAS 9-14301, National Aeronautics and Space Administration, Johnson Space Center, Houston, Tex. (Oct., 1975).

Manuscript received April 26, 1976; revision received August 30, and accepted September 1, 1976.

Methodology for Simultaneous Optimization with Reliability: Nuclear PWR Example

J. R. CAMPBELL
and
J. L. GADDY

Department of Chemical Engineering
University of Missouri-Rolla
Rolla, Missouri 65401

SCOPE

The determination of optimal process reliability can be described as a mixed integer optimization problem. Although not usually included in the optimization study, reliability is an important aspect of process design, affecting both the safety and economics of the installation.

Process reliability can be improved by redundancy (spares), by use of more expensive components (or controls), and by subdividing large units into smaller units that will accomplish the same task. Differing reliability requirements involve new, and sometimes quite different, process arrangements. Improving reliability of a process usually adds to the cost, and this added cost must be offset by better operation.

Reliability can be incorporated in the process study as a constraint that must be met by the process arrangement, or reliability might be built into the cost function as a penalty imposed for less reliable systems. Both of these methods require manipulation of the process arrangement to determine the best configuration. At the same time, however, it is necessary to consider other independent